FULL PAPER

Reversible Soft Top-Contacts to Yield Molecular Junctions with Precise and Reproducible Electrical Characteristics

*Albert Wan, Li Jiang, C. S. Suchand Sangeeth, and Christian A. Nijhuis**

The reproducibility of the electrical characteristics of molecular junctions has been notoriously low. This paper describes a method to construct tunnel junctions based on self-assembled monolayers (SAMs) by forming reversible electrical contacts to SAMs using top-electrodes of a non-Newtonian liquid-metal (GaO_x/EGaIn) stabilized in a microfluidic-based device. A single top-electrode can be used to form up to 15–25 junctions. This method generates SAM-based junctions with highly reproducible electrical characteristics in terms of precision (widths of distributions) and replicability (closeness to a reference value). The reason is that this method, unlike other approaches that rely on cross-bar or nano/micropore configurations, does not require patterning of the bottom-electrodes and is compatible with ultra-flat template-stripped (TS) surfaces. This compatibly with non-patterned electrodes is important for three reasons. i) No edges of the electrodes are present at which SAMs cannot pack well. ii) Patterning requires photoresist that may contaminate the electrode and complicate SAM formation. iii) TS-surfaces contain large grains, have low rms values, and can be obtained and used (in ordinary laboratory conditions) within a few seconds to minimize contamination. The junctions have very good electrical stability (2500 current-voltage cycles and retained currents for 27 h), and can be fabricated with good yields (≈78%).

1. Introduction

Electronic devices based on molecules have already found commercial applications in the form of thin-films in displays,[1,2] organic light emitting diodes,[3–5] or bendable devices.[6–8] Despite these applications, many questions regarding the details of the mechanisms of charge transport across molecules and the molecule-electrode interfaces remain unanswered.[9–13] Molecular electronic devices that are based on single molecules, or self-assembled monolayers (SAMs), are potentially good test-beds to study charge transport across molecules and the molecule-electrode interfaces at the nano-scale.[13,14] The fabrication of such devices is challenging because of the difficulty to form macroscopic-scale electrical contacts to the molecules in non-invasive ways and with minimum numbers of defects in the junctions.[9,13–15] Indeed, the electrical characteristics of molecular junctions with the same molecules differ many orders of magnitude across test-beds (see below).[13]

For molecular electronic devices to become useful in applications, it is important to develop methods to fabricate devices that generate data with high reproducibility in terms of precision, that is, widths of the distributions, and replicability, that is, closeness to a reference value (see Background below). So far, molecular junctions have been incorporated in devices using two configurations: the so-called cross-bar configuration, in which the SAM is sandwiched between two perpendicularly aligned electrodes (**Figure 1**a),[16–21] and the so-called nano- or micropore configuration in which the SAM is formed in a pore on to which the top-electrode is introduced (Figure 1b).[22–27] These two approaches suffer from four (potential) problems that impede the quality of the SAMs and consequently complicate reproducibility across test-beds. i) The bottom-electrode needs to be patterned which normally requires lithography. Patterning by e-beam- or photolithography often leaves resist residues on the electrode behind that are difficult to remove completely and consequently result in defective SAMs.[28–31] ii) The bottom-electrodes contain exposed edges at which SAMs cannot form densely packed layers.[38–40] These edges with defective SAMs are prone to be a source for leakage currents. iii) The bottom-electrodes are prepared by ex situ direct evaporation methods, contain large numbers of grain boundaries at which SAMs cannot pack,[32,33] and risk contamination from ambient.[34,35] iv) The SAMs are exposed to harsh fabrication conductions, for example, ultra-high vacuum conditions and high temperatures during metal deposition steps, or to solvents, that may damage the SAMs, which may results in defective SAMs.[9,36,37]

Here we describe a method to fabricate SAM-based tunnel junctions that generate highly reproducible J(V) data in terms of precision (amongst the best so far;[16,26,32,38–42] see below)

Dr. A. Wan, L. Jiang, Dr. C. S. S. Sangeeth,
Prof. C. A. Nijhuis
Department of Chemistry
National University of Singapore
3 Science Drive 3 117543, Singapore
E-mail: chmnca@nus.edu.sg
Prof. C. A. Nijhuis
Solar Energy Research Institute of Singapore (SERIS)
7 Engineering Drive 1
National University of Singapore
Singapore 117574, Singapore
Prof. C. A. Nijhuis
Graphene Research Centre
National University of Singapore
2 Science Drive 3, Singapore 117542, Singapore

DOI: 10.1002/adfm.201304237

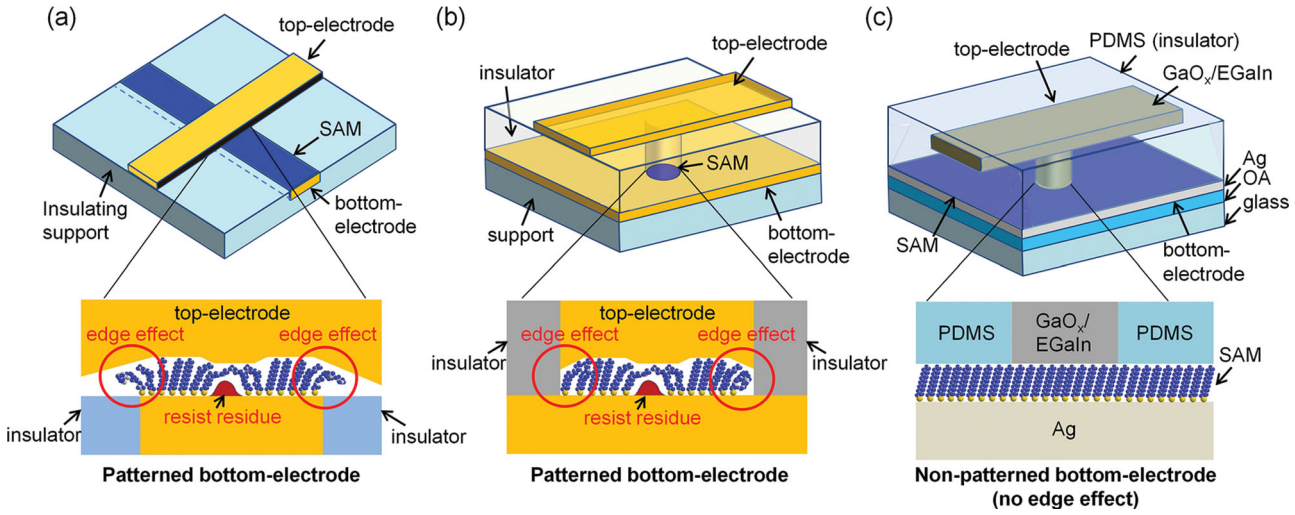

Figure 1. Schematic illustrations of the top- and side views of molecular junctions in a a) cross-bar configuration, b) micro- or nanopore configuration, and c) the configuration reported here that does not require patterning of the bottom-electrode with OA is the optical adhesive (see Experimental Section).

and accuracy (relative to other "EGaIn"-based techniques; see below), in good yields of working junctions, with a value of the tunneling decay coefficient β close to the consensus value, and good electrical stability. This method works well because it i) does not require patterned bottom-electrodes, ii) is compatible with ultra-flat template stripped bottom-electrodes that contain large grains, iii) does not expose the SAMs to harsh fabrication conditions, and iv) minimizes potential contamination of the bottom-electrode from the ambient. These improvements in the fabrication process resulted in SAM-based junctions of high quality and reproducibility that are (nearly) independent of the users or top-electrodes.

By far most studies have focused to develop techniques to maximize yields of working junctions, or to produce them on large scales, but the reproducibility of the systems has been rarely defined and reported.[43] It is well-known that some electronic properties of SAMs have been reproduced across several test-beds, but with a large spread in the current densities of eight to nine orders of magnitude.[13,16,46] The width of the distributions indicates the precision of the data. The closeness of the average value of the distribution to a reference value, or standard value, indicates the accuracy (see **Figure 2** and Background below).[44] Standards for electrical characteristics across test-beds have not been defined because often standards have not been established within a single laboratory or, for a given technique, across different laboratories.[45,46] Here we do not wish to establish standard values for the electrical characteristics of junctions across test-beds, but we determine the replicability of our measurements against other "EGaIn"-based techniques.

Weiss et al.[35] reported that clean template-stripped (TS) metal surfaces are ultra-flat (three to four times lower root-mean-square (rms) surface roughness than the surfaces fabricated by direct metal deposition) and readily available in ordinary laboratory conditions: the metal surface can be stripped off the template and immediately (within a few seconds) immersed into a solution with the SAM precursor to minimize contamination from the ambient environment. The authors showed that these TS metal surfaces resulted in SAM-based junctions in higher yields and a smaller spread in the J(V) data than those junctions formed with bottom-electrodes obtained by direct metal deposition.[32] Hence, a fabrication technique to construct SAM-based devices that is compatible with TS surfaces, that is, a technique that does not require patterning of the bottom-electrode, is highly desirable.

Cone-shaped tips of a liquid-metal alloy (eutectic mixture of 75.5% Ga and 24.5% In by weight with a thin 0.7 nm surface layer of conductive GaO_x, abbreviated as GaO_x/EGaIn)[47] have been used to form electrical contacts to SAMs in various physical-organic studies of charge transport across SAMs.[16,17,40,47–59] This method (in the hands of an experienced user) produces highly reproducible data in good yields and is very easy to set-up in a laboratory (see Background). This method has also disadvantages and it suffers from user dependent variations in the details of the formation of tips and the SAM//GaO_x/EGaIn contacts, and the stability of the junctions is limited by the

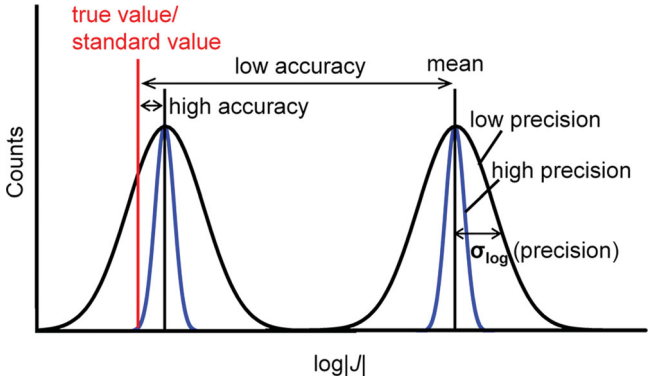

Figure 2. Schematic illustration of the definition of the accuracy and precision (σ_{log}) of the electrical measurements for SAM-based junctions. This diagram is derived from similar diagrams discussed in reference.[44]

Table 1. The average values of log|*J*|, β, and J_0, measured using different EGaIn-based techniques for n-alkanethiolate SAMs.

Techniques	<log|*J*|> [A cm^{-2}]					β [n_C^{-1}]	J_0 [A cm^{-2}]
	SC_9CH_3	$SC_{11}CH_3$	$SC_{13}CH_3$	$SC_{15}CH_3$	$SC_{17}CH_3$		
this work	−1.95	−2.92	−3.63	−4.63	−5.44	1.00 ± 0.03	2.4×10^2
tips[a)]	−1.77	−2.47	−3.70	−4.32	−5.31	1.02 ± 0.09	3.4×10^2
modified tips[b)]	−1.250	−1.60	−2.30	−3.270	−4.10	0.91 ± 0.02	25×10^2
cross-bar[c)]	NA	−2.70	−3.20	−4.50	−5.20	0.92 ± 0.24	3.4×10^2
Reference values[d)]	−1.7 ± 0.4	−2.4 ± 0.6	−3.2 ± 0.6	−4.2 ± 0.6	−5.0 ± 0.6	1.00 ± 0.02	$0.2 - 2 \times 10^3$

[a)]These values were taken from the literature;[40] [b)]These values were taken from the literature;[46] [c)]These values were taken from the literature;[16] [d)]See the text for details.

details of the micromanipulator on which the top-electrode is mounted.

Here we describe a new type of top-electrode that allows us to form molecular junctions without the need for patterning of the bottom-electrode that is compatible with metal surfaces obtained by TS (Figure 1c). The GaO_x/EGaIn was stabilized in a microfluidic device made of a transparent rubber of polydimethylsiloxane (PDMS) which we placed on the SAMs. After electrical examination of the junctions, we removed the top-electrode from the SAM and placed it in contact with a different area of the SAM, or with a SAM on a different substrate, to form a new junction. Our method produces *J*(V) data that are very similar to data obtained by other EGaIn-based techniques, and are independent of temperature, from which we conclude that coherent tunneling dominates the mechanism of charge transport (see **Table 1** and Background).[16,40,46] The advantages of this method is that encapsulation of the metal top-electrodes in PDMS eliminates instabilities associated with micromanipulators, e.g., drift or vibrations, and minimizes user-to-user variations in the details of the formation of the top-electrode and the SAM//GaO_x/EGaIn contacts (see Background) resulting in data with high precision and replicability (see Background). These features made it possible to study the electrical characteristics of the junctions over a period of time of ten days, bias stressing up to 1.0×10^5 s, and over the range of temperatures of 160 – 297 K (we did not optimize the devices to maximize the temperature range). Cone-shaped tips of GaO_x/EGaIn can only be prepared one at a time per "EGaIn-set-up", while the fabrication process reported here can be performed in parallel to fabricate large numbers of junctions (we did not try to fabricate more than roughly 100 junctions per day). In addition, we identify several sources of error that cause scattering of the data; these sources of error are likely also present in the other test-beds and should be taken into consideration in future experiments.

2. Background

2.1. Junctions with GaO_x/EGaIn Top-Electrodes

The EGaIn spontaneously forms a self-limiting layer of GaO_x in air with a thickness of 0.7 nm[47] and because of its non-Newtonian properties this material can be shaped.[47,60–62,64] Therefore, unlike Hg, GaO_x/EGaIn forms stable structures in PDMS micro-channels.[64,65] The oxide layer also prevents the bulk EGaIn from alloying with the gold or silver bottom-electrode which adds stability to junctions. The oxide layer is defective and contains oxygen vacancies,[47] and it is highly conductive.[46]

The precision of the data, that is, the width of the distributions of the values of *J* (see Figure 2 for definitions), generated using junctions formed with cone-shaped tips of GaO_x/EGaIn relies on the operator because the formation of the tips and bringing the tip in contact with the SAMs are usually performed with a manually operated manipulator. (Chiechi et al.[49,55] use piezo-controlled manipulators). For instance, the contact size, tip roughness, and the speed of the tip used to approach the SAMs, differ in details from user-to-user.[43,56] Whitesides et al.[43,56] showed that these factors broaden the distributions of the current densities significantly. Recently, Whitesides et al.[46] reported that flattening the cone-shaped tips by molding the tips against flat and clean Si/SiO_2 surfaces followed by voltage cycling (three cycles of ±2 V) resulted in smoother tips and higher reproducibility between users than using unmodified cone-shaped tips of GaO_x/EGaIn. Stabilization of the GaO_x/EGaIn in a micro-channel in a cross-bar configuration resulted in well-defined geometrical contact areas, but the improvement in the width of the distributions of the values of *J* was only marginal because the bottom-electrodes contained edges at which SAMs cannot pack well.[16,17,67]

Despite the (small) differences between the details of the formation of the GaO_x/EGaIn top-contacts, Table 1 shows that the *J*(V) characteristics of SAM-based junctions with GaO_x/EGaIn top-electrodes across laboratories differ slightly (less than one order of magnitude) compared to the eight to nine orders of magnitude difference in *J*(V) characteristics across test-beds. Thus "EGaIn"-based techniques produce data that are replicable (in spite of the different levels of precision) across laboratories and platforms.

2.2. Precision and Accuracy

According to Equation (1) (see below), the values of log|*J*| are normally distributed when the error in *d* follows a normal distribution because *J* depends exponentially on *d*.[43,56] The error

in d certainly depends on many factors including defects in the electrode materials, for example, step edges, vacancy islands, or grain boundaries, defects in the SAMs,[32,68] for example, phase domains,[69] physisorbed or chemisorbed materials,[24,34] or errors during the fabrication process, for example, (partial) penetration of the SAMs by the top-electrode,[70,71] or damage to the SAMs inflicted by solvents[72,73] or high temperatures during fabrication.[26] These potential defects that result in uncertainties in the effective values of d and all may result in batch-to-batch or user-to-user variations and consequently introduce error that cause the data to deviate from Gaussian distributions and increase the standard deviation. Thus, one way to compare the precision of different techniques for junction measurements is to compare the standard deviations (σ) of the values of J for normal distributions, or the analogues log-standard deviations (σ_{log}) for log-standard distributions (Figure 2). Data that follow narrow distributions make it possible to separate informative data from non-informative data more accurately than those data that follow broad distributions.

As shown in Figure 2, the accuracy of the data is defined as the difference between the data obtained from the measurement and the true, or defined, value.[44] This Figure shows that data may be very precise but not accurate, but all other combinations are also possible and, for instance, data may be accurate but not precise.[44] Although the width of the histograms of the values of J may be very narrow for a given test-bed, they do so with values that differ by eight to nine orders of magnitude across different test-beds.[13,16,46] In this paper, we do not aim to define the standards for the absolute values of J_0 for junctions with SAMs of n-alkanethiolates because the factors that contribute to J_0 for a given test-bed have, in general, not been identified. Here we wish to establish the replicability of our method relative to "EGaIn"-based techniques[16,40,46] using reference values of the current densities (Table 1). This comparison helps to identify sources of error that are important to consider in general to maximize both precision and replicability (see below).

2.3. Error Analysis

As mentioned above, normally the values of log|J| (for a given voltage) are plotted versus n_C followed by fitting this data to the Simmons equation. Reus et al.[43] compared different statistical methods to determine the values of β and J_0 and discussed the differences and limitations of these methods thoroughly. These methods either used average values of log|J| (Gaussian mean, median, or arithmetic mean) to which a line was fitted using a least-squares fitting algorithm, or by plotting all data to which a line is fitted using either a least-squares algorithm or by minimizing the sum of the absolute error. Here we chose two methods to determine the values of β and J_0: i) plotting the Gaussian means of the value of log|J| vs n_C followed by least squares fitting of Equation 1 (method 1) and ii) plotting all data (all values of log|J| except data that was obtained for junctions that shorted) followed by fitting to Equation (1) by minimizing the sum of the absolute values of the error (method 2). The first method assumes the data follow random distributions, or, in other words, the data are normally distributed, while the second method does not make any assumptions regarding the type of distribution.

3. Results and Discussion

3.1. Fabrication of the Top-Electrode

Figure 3 shows the fabrication process of the top-electrode of GaO_x/EGaIn stabilized in a microfluidic chip made of PDMS. We fabricated the mold to shape the PDMS which consisted of a pillar (with a height of 60 μm and the diameter of ≈45 μm) connected to a line (1.0 cm × 10 μm × 10 μm; Figure 3a) via a two-step photolithography process (see page S4 and Figure S1, Supporting Information, for more details) following a previously reported procedure.[63] **Figure 4**a shows a scanning electron micrograph (SEM) of the mold. The image shows that the pillar had a larger base-diameter (55 μm) than top-diameter (35 μm) and had a depression at top-center due to over-developing of the thick layer of photoresist during the lithography process.

The mold was treated with 1H,1H,2H,2H-perfluorooctyltrichlorosilane ($Cl_3Si(CH_2)_2(CF_2)_5CF_3$, FOTS) to minimize the interaction of the PDMS with the wafer to ensure the defect free separation of the PDMS from the mold (see below). A layer of 20 μm of uncured PDMS (Sylgard 184) with curing agent (in a ratio of 10:1) was formed by spin-coating which covered the line but not the pillar (Figure 3b). After curing of the PDMS at 80 °C for 30 min, we spin coated an additional layer of 5 μm uncured PDMS (with curing agent) and aligned a channel (channel 1) in PDMS (1.0 cm × 300 μm × 120 μm), which we fabricated in a separate step (see the Supporting Information), with an inlet and an outlet over the pillar perpendicularly with respect to the line of the mold (Figure 3c). A covalent seal was formed between the layers by curing the 5 μm thick PDMS layer at 80 °C for 30 min. This thin PDMS layer improved the mechanical stability of the devices. We added more uncured PDMS with curing agent to stabilize the 20 μm PDMS film (Figure 3d). After curing the PDMS, we separated the microfluidic chip which contained two perpendicular channels with a microscale through-hole at the intersection from the mold and punched a hole at the end of the channel 2 (Figure 3e). Figure 4b shows the optical micrograph of the cross section of the PDMS device (without liquid metal in the micro-channels) and that the 3D structures were successfully replicated by the PDMS.

To inject GaO_x/EGaIn into the micro-channel 1 and the through-hole, we placed the microfluidic chip on indium tin oxide (ITO). The transparent and conductive properties of ITO allowed us to follow all subsequent stages of the fabrication process by optical microscopy and conductivity measurements. Channel 1 was filled with EGaIn by applying vacuum (≈500 Torr) to the outlet of the channel with a drop of GaO_x/EGaIn present at the inlet (Figure 3f), after which we applied vacuum to channel 2 to fill the through-hole with GaO_x/EGaIn (Figure 3g). The diameter of channel 2 was chosen so that the high surface tension of GaO_x/EGaIn (624 mN/m) prevented it to fill this channel in the range of the applied pressures.[64,65] Figure 4c shows that the liquid-metal did fill the through-hole but not channel 2. We derived the geometrical contact area of

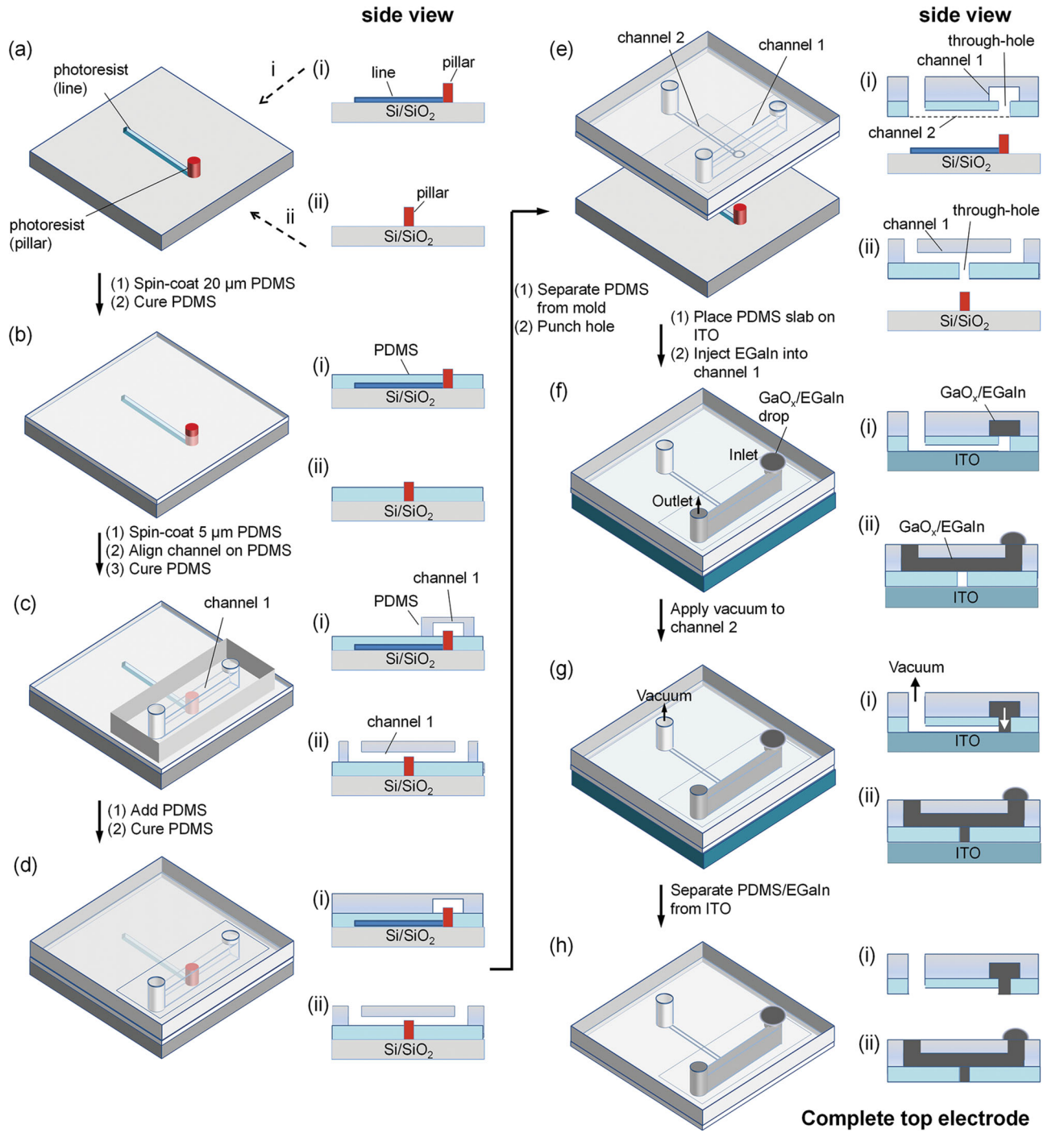

Figure 3. Fabrication of the top-electrode. a) The mold consists of a line and a pillar on a Si/SiO_2 wafer with a layer of FOTS (FOTS is not indicated for clarity). b) A layer of PDMS (20 μm) was spin-coated on the mold to fully cover the photoresist line, but not the pillar, and cured. c) A thin layer of PDMS (5 μm) was spin-coated on the first layer of PDMS and channel 1 in PDMS was aligned over the pillar perpendicularly with respect to the line of the mold. The thin layer of PDMS was cured. d) More uncured PDMS was added to stabilize the thin layer of PDMS and cured. e) The microfluidic device was peeled off from the mold and a hole was punched at the end of the small channel. f) We placed the microfluidic device on an ITO substrate and injected GaO_x/EGaIn into the PDMS channel. g) The through-hole was filled with GaO_x/EGaIn by applying vacuum to channel 2. h) Separation of the microfluidic device from the ITO yielded a complete top-electrode.

the GaO_x/EGaIn with the ITO from these images. We found that the diameter of the GaO_x/EGaIn-ITO contact (35 μm) was smaller than the diameter of the through-hole (55 μm) because of a gap of ≈10 μm between the GaO_x/EGaIn and the walls of the hole. The formation of the gap was likely caused by the high surface-tension of the GaO_x/EGaIn. By simply measuring the resistance between the ITO and the GaO_x/EGaIn present at the inlet using a multi-meter, we determined if the GaO_x/

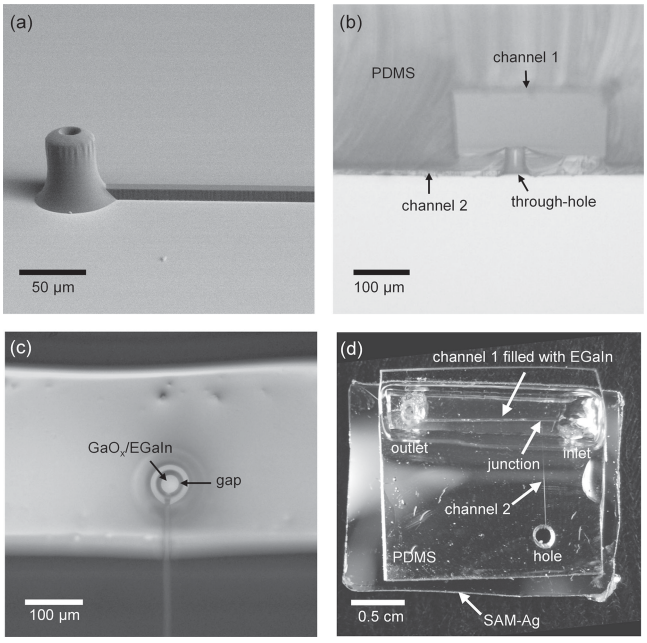

Figure 4. a) A SEM image of the mold recorded from an angle with respect to the surface normal of 25°. b) Optical micrographs of the cross section of the PDMS micro-channel, and c) of the PDMS micro-channel with GaO_x/EGaIn in the through-hole. d) Photograph of a complete device.

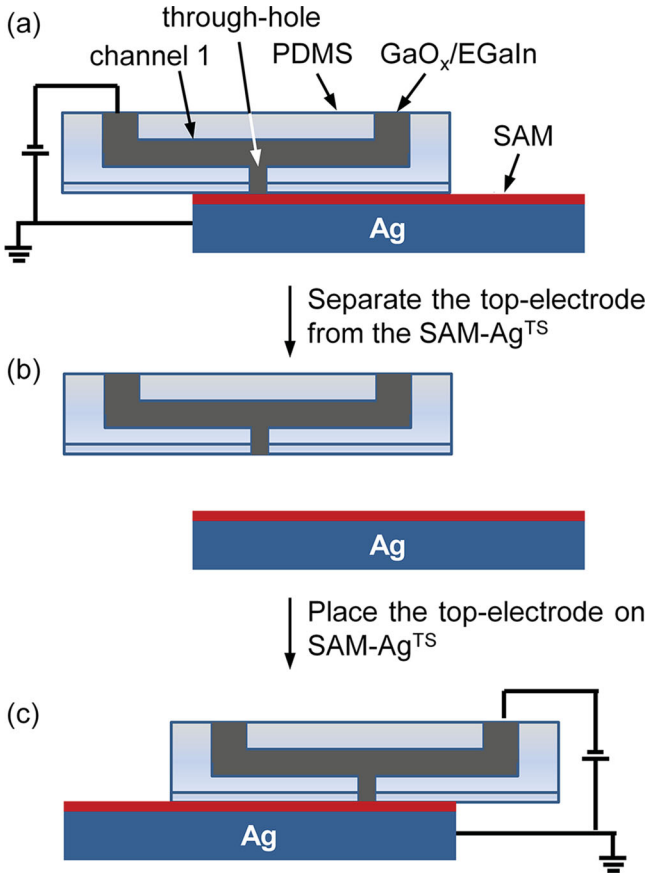

Figure 5. The procedure of forming reversible contacts to the SAMs. a) Placement of the top-electrode on the SAM-Ag^{TS} substrate allows the GaO_x/EGaIn in the through-hole to form contacts with the SAM. b) After completing the *J*(V) measurements of one junction, we separated the top-electrode from the SAM-Ag^{TS} substrate and c) placed it on a different area of the SAM-Ag^{TS} substrate, or on a different substrate, to form a new junction.

EGaIn filled the through-hole and formed good electrical contact with the ITO. Finally, we separated the top-electrode from the ITO (Figure 3h). During this step, no liquid-metal was left behind on the ITO surface.

We note that the lengths of the channels 1 and 2 were arbitrarily chosen. If required, the dimensions of the top-electrodes can be easily reduced by reducing the lengths of channels 1 and 2. Figure S2 shows a top-electrode but now with both channels 1 and 2 with a length of 0.5 cm.

3.2. Fabrication of the Junctions

Figure 5 shows schematically the reversible placement of the top-electrode on a SAM on Ag^{TS} electrodes (Figure 5a). We found that the electrodes formed good electrical contacts with the SAMs in most cases; in cases a good contact did not form (which resulted in either an open circuit or *J*(V) characteristics with values of *J* that were more than two orders of magnitude lower than the log-mean value), we simply applied vacuum to channel 2 to restore good electrical contact of the GaO_x/EGaIn with the SAM. Figure 4d shows a photograph of a complete device. The PDMS is flexible and forms a reversible conformal contact with the substrate through van der Waals interactions.[66] We observed that the seal between the top-electrode and the SAM-Ag^{TS} substrate allowed the GaO_x/EGaIn to form good electrical contacts with the monolayers. Because the EGaIn surface is exposed to air in our experiments, we believe that the GaO_x film that forms spontaneously in air on the bulk metal is continuous and very similar in composition to that in other types of EGaIn-based junctions (see Background). After recording the *J*(V) curves, we separated the top-electrode from the substrate (Figure 5b), and placed it in contact with the SAM in an area that had not been in contact with either the PDMS (to avoid potential contamination of the SAMs by, for instance, low molecular weight or uncured PDMS) or the GaO_x/EGaIn previously, or in contact with another Ag^{TS}-SAM substrate (Figure 5c).

The procedure to remove the top-electrode from the surface and to form a new junction typically takes 5–10 s. The rate at which junctions can be formed for a single electrode is similar to that for cone-shaped based techniques (once a cone-shaped tip of GaO_x/EGaIn has been formed). We used 4″ wafers which allowed us to prepare six top-electrodes at once per wafer, but top-electrodes with shorter channels can also be prepared (see SI) to yield for instance 18 top-electrodes per wafer. The top-electrodes lasted for about 15–25 junctions before they failed and did not form good electrical contacts with the SAMs. Optical micrographs of these failing top-electrodes revealed that the small channels were blocked by dust particles and therefore good contacts could not be restored by applying vacuum

to channel 2. Occasionally (in about 1 out of 20 top-electrodes), the thin PDMS membrane surrounding the GaO_x/EGaIn ruptured resulting in ill-defined junction areas. Hence, the number of junctions that can be formed in parallel is only limited by the number of available molds and the rate of data acquisition is only limited by the electronic equipment.

3.3. Proposed Reference Values of *J* for EGaIn-Based Techniques

Table 1 shows the values of <log|*J*|> for Ag^{TS}-SC_n//GaO_x/EGaIn junctions with n = 10, 12, 14, 16, and 18 reported in the literature[16,40,46] and reported here. The reference values of <log|*J*|> were obtained by averaging the values of <log|*J*|> from references[16,40,46], and this work. We determined reference values of β and J_0 by least squares fitting the average values of <log|*J*|> to the Simmons equation (see **Figure 6** and discussion below). The values of J_0 depend on many factors, including the effective contact area or contact resistance, as explained in detail by Whitesides et al.;[46] here, we do not aim to compare the absolute values of J_0 across test-beds but only across "EGaIn"-based techniques. As we show here, these proposed reference values are useful to compare "EGaIn"-based techniques to each other, or to identify sources of error.

3.4. The Electrical Characteristics of the Devices

In molecular electronics, it is a common practice to determine the tunneling decay coefficient, β (n_C^{-1}), by measuring the value of J at a given voltage, V (V), as a function of the thickness of the SAMs, d (Å or n_C which is the number of carbon atoms in the back bone of the molecules), when through bond tunneling is the dominant mechanism of charge transport.[9,13,14] By fitting the data to the Simmons equation (Equation (1)), one can derive the values of β and of the hypothetical current density, J_0 (A cm^{-2}), for a junction with d = 0. This procedure has been used across several test-beds using SAMs of n-alkanethiolates of the form $S(CH_2)_{n\text{-}1}CH_3$ and it is now commonly believed that the correct value for β is 1.0 n_C^{-1}.

$$J = J_0 e^{-\beta d} \quad (1)$$

We formed junctions with SAMs of $S(CH_2)_{n-1}CH_3$ (n = 10, 12, 14, 16, or 18) on Ag^{TS}. Prior to the self-assembly of the monolayers, we purified the n-alkanethiolates (see the Supporting Information). Although we did not test the performance of the junctions as a function of thiol purity, this procedure minimizes potential variations in the batch-to-batch quality of the thiols as received from the suppliers which could influence replicability

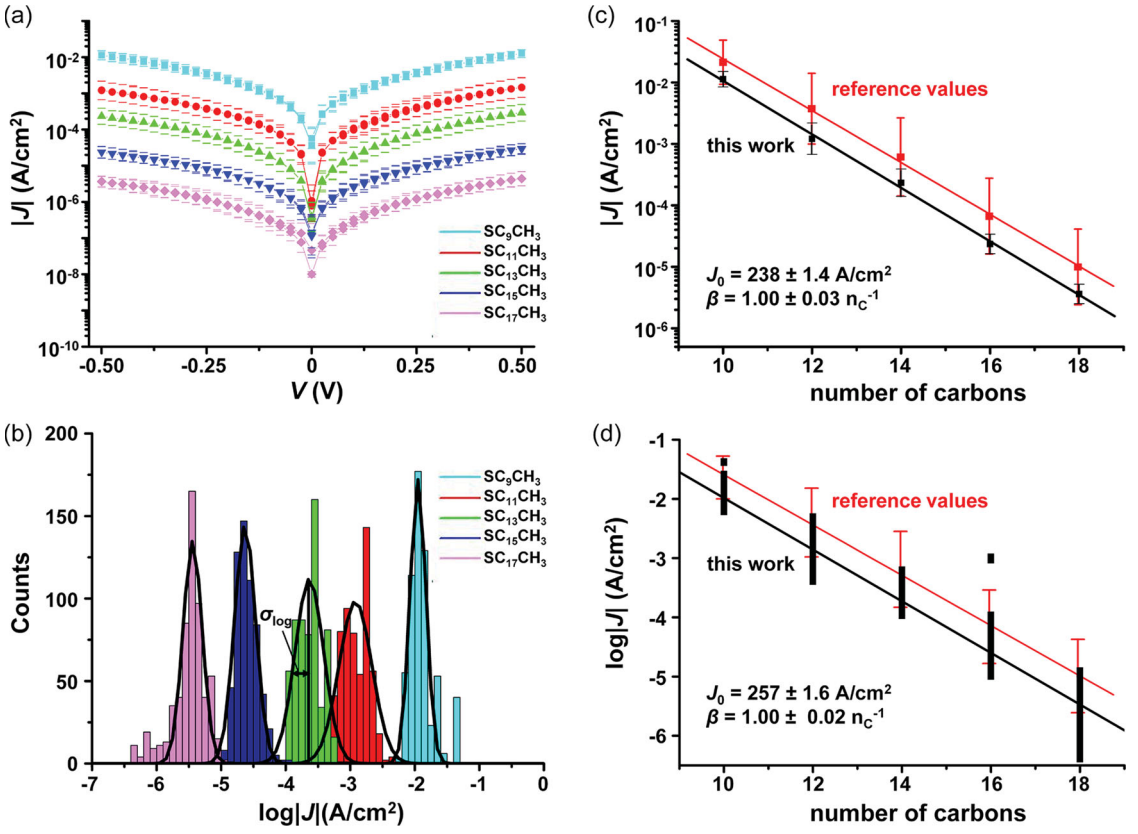

Figure 6. a) Plots of <|*J*|> vs *V* and b) histograms of log(|*J*|) at –0.50 V with Gaussian fits. The log-mean |*J*| as a function of the number of carbons measured at –0.50 V (black symbols) with a fit to Equation 1 (black line) using method 2 (see page S4, Supporting Information); c) Plots of all data of log|*J*| at –0.50 V versus chain length and d) the trend line fitted by using the least-absolute-errors algorithm using method 2 (see page S4, Supporting Information). The red lines and symbols in panels c and d represent the reference values as explained in the text.

Table 2. The total number of non-shorting junctions (N_J), the yields of the working devices and σ_{log} of J(V) measurements for the n-alkanethiolate-based junctions.

Molecules	Junctions	N_J	Non-shorting junctions	Non-shorting yield [%]	σ_{log}
SC_9CH_3	21	600	15	71	0.12
$SC_{11}CH_3$	19	600	15	79	0.25
$SC_{13}CH_3$	20	600	15	75	0.22
$SC_{15}CH_3$	19	600	15	79	0.16
$SC_{17}CH_3$	17	600	15	88	0.15
total	96	3000	75	78[a]	0.18[a)]

[a]These numbers are average values.

and/or precision of the electrical characteristics of the junctions. Using a single top-electrode, we measured a complete graph of $|J|$ against n_C determined at –0.50 V as follows. We recorded the values of J over the range of biases of –0.50 and 0.50 V (one trace ≡ 0 V → 0.50 V → –0.50 V (2) 0 V) at intervals of 25 mV. We recorded a total of 20 J(V) traces for each junction and measured three junctions for each type of SAM using a single top-electrode. Thus, we formed 15 junctions with five different SAMs and recorded in total 300 traces and 600 values of $|J|$ at each applied bias using a single top-electrode. This procedure was repeated with five different top-electrodes to yield a total of five plots of versus n_C operated by one out of three different users. This procedure allows us to determine the replicability and precision of data across individual users and top-electrodes.

Table 2 summarizes the characteristics of the junctions. We excluded shorts and open circuits and kept the number of working junctions constant so the data for all junctions carry the same weight in our analysis. Figure 6 shows the averaged J(V) curves over all users for each type of junction, the histograms of log|J| at –0.50 V, and plots of <|J|> versus n_C. Fitting the data to the Simmons equation gave values of β of 1.00 ± 0.03 n_C^{-1} and J_0 of 2.4 × 10^2 A cm^{-2} (using method 1; see Supporting Information). We note that the value of J_0 is not precise because of the long extrapolation.[43,46] The value of β is very close to the consensus value,[16] and the value of J_0 is very close to previously reported values obtained for other types of junctions with GaO_x/EGaIn top-electrodes (See **Table 3** and below).[16,40] These results indicate that the dominant mechanism of charge transport across our junctions is through-bond tunneling.

One may argue that if the distribution of log|J| deviates from normality, it is more accurate to estimate trend statistics by fitting all values of log|J| by a least-absolute-errors algorithm (see method 2 described on page S4) rather than by fitting Gaussian means of log|J| with a least-squares algorithm (method 1) since the former method does not assume any type of distribution while the latter method does.[43] Figure 6d shows the plot of all values of log|J| at –0.50 V versus n_C with a fit to the Simmons equation using method 2. The values of β and J_0 were found to be 1.00 ± 0.02 n_C^{-1} and 257 ± 1.6 A cm^{-2}, respectively. Considering the small differences in the values of β and J_0 obtained by methods 1 and 2, we believe that the assumption that our data follow a normal distribution introduces a negligibly small error in the analysis of our data.

3.5. Precision of the Data

The striking difference of the current fabrication method with respect to other methods is that the values of log-standard deviation (σ_{log}) are very small and fall in the range of 0.12 to 0.25 with an average of 0.18 ± 0.05; these values are one of the lowest in general (Table 3). Thus our method generates J(V) data with very high precision.

To determine reproducibility between different top-electrodes and different investigators we performed two experiments: three investigators measured the electrical characteristics of the junctions using i) five different top-electrodes each operated by one of the three investigators, or ii) one top-electrode operated by all three investigators. **Figure 7** shows the corresponding five plots of log|J| versus n_C^{-1} determined by three different users using five different top-electrodes. Each plot was measured by one user and top-electrode combination as indicated in the Figure. Figures S4–S8 (Supporting Information) show the corresponding histograms of log(|J|) determined at –0.50 V for all Ag^{TS}-SC_n//GaO_x/EGaIn junctions for each user and top-electrode combination. The values of

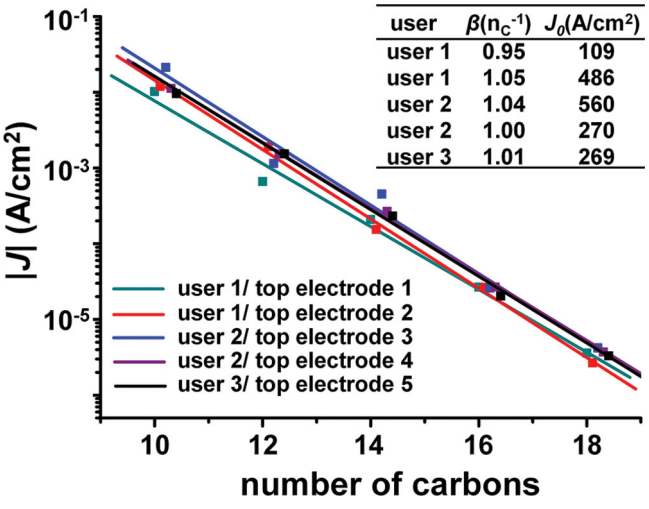

Figure 7. Plots of |J| versus chain length of the n-alkanethiolates at –0.50 V obtained by three different users using five different top-electrodes. The data are offset by 0.1 carbon number for clarity. The inset shows the values of β and J_0 and the solid lines are fits to the Simmons equation.

Table 3. Comparison of σ_{log}, β, and yield of different tunneling junctions with SAMs.

Type of junction	Technique	N	σ_{log}	β [n_C^{-1}]	yield [%]	N_{max} [k)]	Refs.
Ag-SAM//SAM-Hg	Hg-drop	1–5	≈1.0–1.5[c)]	0.80	NA	13	[32]
Hg-SAM//Hg	Hg-drop	5–10	≈0.11–0.60[c)]	1.06 ± 0.04	NA	10	[38]
Hg-SAM//SAM-Hg	Hg-drop	5–10	≈0.11–0.43[c)]	1.02 ± 0.07	NA	10	[38]
Si-SAM//Hg	Hg-drop	>7	≈0.37–0.70[c)]	0.76 ± 0.09	NA	NA	[88,97]
Al/Al_2O_3-SAM//Hg	Hg-drop	12–18	0.25–0.75	1.34 ± 0.004[h)]	25–75	18	[41]
M-SAM//M[a)]	CP AFM	5–10	≈0.28–1.0[c,d)]	1.1	NA	10	[42]
Au-SAM//Au	STM break junction	3000	0.02–10[d)]	0.94–0.96	10–40	NA	[94]
Ag-SAM//Ag	STM break junction	7000	≈0.16–0.32[f)]	0.98 ± 0.05[i)]	NA	NA	[95]
Au-SAM//Au	nanoskiving	>10	≈0.05–0.28[c)]	0.94	36–67	32	[85]
Si-SAM//Au	PALO[b)]	>10	≈0.05–0.26[c)]	NA	NA	NA	[92]
Si-SAM//Au	flip chip lamination	>30	≈0.06–0.1[c,g)]	NA	90	NA	[89]
Au-SAM//Au	crossed-wires	NA	≈0.22[c,e)]	NA	NA	NA	[90]
Au-SAM//polymer/Au	PEDOT:PSS /micropore	>17	≈0.11–0.15[c)]	0.71 ± 0.06	>95	100	[93]
Au-SAM//polymer/Au	PEDOT:PSS/micropore	74	≈0.23[c)]	1.33 ± 0.05	58	74	[39]
Au-SAM//Au	SiO_2 micropole	33–63	0.23–0.527	1.04–1.08	1.2–1.75	NA	[26]
Au-SAM//Au	Si_3N_4 nanopore	≈160	≈0.27–0.32[c)]	1.07 ± 0.02	7.1	NA	[14]
Au-SAM//Au	wedging transfer	200–340	0.57–1.13	0.73 ± 0.06	38–50	NA	[86]
Au-SAM//graphene/Au	graphene/micropore	258	≈0.27–0.67[c)]	1.06 ± 0.14	90	2000	[87]
graphene-SAM// graphene	graphene//micropore	>50	≈0.17–0.35[c)]	0.54 ± 0.01	>80	NA	[91]
Ag-SAM//GaO_x/EGaIn	cone-shaped tip	376–3892	0.23–1.1	1.04 ± 0.06[j)]	82–100	NA	[40]
Ag-SAM//GaO_x/EGaIn	Flattened cone-shaped tip	360–480	0.3 – 0.7	0.92 ± 0.02	≈90%	NA	[46]
Ag-SAM//GaO_x/EGaIn	cross-bars	400–756	0.21–0.85	0.98 ± 0.2	70–85	NA	[16]
Ag-SAM//GaO_x/EGaIn	through-hole	600	0.12–0.25	1.00 ± 0.03	78	2500	this work

[a)]A metal-coated (Au, Ag, or Pt) AFM tip was contacted with a SAM on a Au-, Ag-, or Pt-coated Si substrate; [b)]Polymer-assisted lift-off method; [c)]Roughly estimated from the J(V) curves in the corresponding references; [d)]The log standard deviations of the resistance instead of current density were measured; [e)]The standard deviations of the conductance instead of current density were reported; [f)]The log standard deviations of the conductance instead of current density were reported; [g)]The standard deviations of the current at 1 V instead of current density were reported; [h)]This value was reported for C8-C12 junctions. The value was reported to be 0.77 ± 0.005 for the junctions of C12-C16; [i)]The β value was measured to be 0.93 ± 0.05 n_C^{-1} when the Au tip was used to measure the junctions of SAMs on Au substrates; [j)]This value was obtained by measuring the SAMs of n-alkanethiolate with even number of carbons in the molecules. The value of β was found to be 1.19 ± 0.08 n_C^{-1} for SAMs of n-alkanethiolate with odd number of carbons in the molecules; [k)]The maximum number of continuous scans without shorting or becoming open circuit for a single junction. These numbers are either shown or indicated in the papers.

β obtained from these plots were all in the range of 0.95–1.05 n_C^{-1} with values of J_0 ranging from 109–560 A cm^{-2} (see inset of Figure 7). Note that we give a range of values rather than standard deviations because the number of J(V)-curves is per user lower than the total number of data; these numbers are not precise but reasonably replicable because they all are in the range of previously reported values of 0.2–2 × 10^3 A cm^{-2} (Table 1).

To investigate if the data depend on the users, we also examined the histograms of the values of log|J| at –0.50 V for junctions with SAMs of $SC_{17}CH_3$ obtained by three different users using the same top-electrode. Figure 7 shows that the data are independent of the user who conducted the measurement. These results indicate that the values of log|J| and β are narrowly distributed and independent of the user or top-electrode: the data produced by our technique is precise with respect to different operators and top-electrodes.

3.6. Replicability of the Data

As mentioned in the Introduction, Weiss et al.[32] reported that junctions with TS bottom-electrodes result in junctions with higher yields in non-shorting junctions with smaller log-standard deviations than those junctions with direct metal deposited bottom-electrodes, but the authors did not discuss whether the topography of the bottom-electrode is important in the replicability of the data. To determine if the topography of the bottom-electrode is an important source for lowering the replicability, we formed SAMs of $SC_{17}CH_3$ (using the same batch of the thiol precursor) on as-deposited Ag substrates, which had a rms roughness of 3.3 nm and small grains of < 3 × 10^{-2} μm^2, and on TS surfaces, which had a rms roughness of 0.9 nm and large grains of 0.05–0.9 μm^2 in agreement with previously reported data (see Supporting Information Figure S3 for AFM images).[32,35] Subsequently,

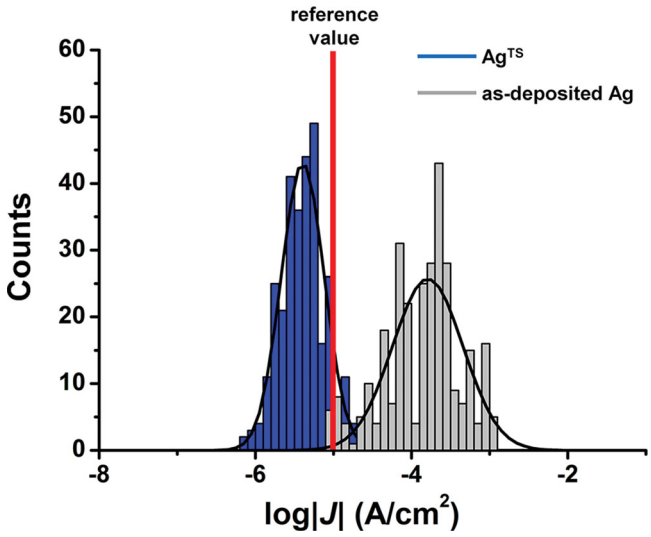

Figure 8. Histograms of $|J|$ determined at –0.50 V for junctions with $SC_{17}CH_3$ SAMs supported by as-deposited Ag substrates and that for junctions with Ag^{TS} substrates. The red vertical line indicates the reference value of log|J| for these junctions.

we formed junctions using one top-electrode operated by one investigator. **Figure 8** shows that the values of J increased nearly two orders of magnitude and the σ_{log} increased from 0.26 to 0.58 as we changed the bottom-electrode from Ag^{TS} to as-deposited Ag. This change in the topography of the bottom-electrode resulted in large decrease in the precision and replicability of the J(V) data. The exact rms values and grain sizes of the bottom-electrodes depends on many factors including deposition rate, base-pressure of the vacuum chamber, pretreatment of the target surface, and so forth. Thus, small variations in the topography of the bottom-electrode can be a source of data broadening and may cause shoulders or even new peaks in histograms of J. To maximize the precision and replicability of the J(V) data generated by our method, we record AFM images for every new batch of electrodes and only use surfaces similar to that shown in Figure S3a before we start experiments.

To show that stabilization of the GaO_x/EGaIn in the through-hole in PDMS contributes to the precision of the data, we measured the J(V) characteristics of junctions with SAMs of $SC_{17}CH_3$ with top-electrodes of GaO_x/EGaIn stabilized in PDMS (**Figure 9**a) or with cone-shaped tips of GaO_x/EGaIn operated by three investigators (Figure 9b). Figure 9 shows that both data sets have their log-mean value of J close to the reference value. The widths of both distributions are comparable, but shoulders on both sides of the main peak are visible which mainly originated from one of the three operators for junctions with cone-shaped tips of GaO_x/EGaIn. Thus, in this experiment user-to-user correlation was significant. These results are similar to those reported by Reus et al.[16] who collected large values of N_J of up to a few thousand by multiple investigators and reported broad distributions that contained multiple peaks. Junctions prepared with cone-shaped tips of GaO_x/EGaIn vary in details of the formation of the tip and the formation of the junctions that differ from user-to-user (see Background section). The stabilization of the top-electrode in microfluidic device minimizes the user-to-user variations in the formation of the top-electrodes, the geometric area of the junctions, and the potential error associated with vibrations and drift of the cone-shaped tip of GaO_x/EGaIn mounted on a micro-manipulator as top-electrodes resulting in precise data.

3.7. Stability of the Devices

To ensure our test-bed can be used as a reliable platform for studying charge transport across SAMs, it is crucial to know the electrical stability and the lifetime of these devices. We tested the electrical stabilities of the devices incorporating SAMs of SC_9CH_3, $SC_{13}CH_3$ and $SC_{17}CH_3$ against continuous cycling of voltage (2500 cycles of 0 V → 0.50 V → –0.50 V → 0 V), bias stress (by applying a constant bias of –0.50 V for 10^5 seconds), and aging (ambient conditions at room temperature) over a period of time of ten days. **Figure 10**a shows that these devices are electrically stable and did not short during voltage cycling. Figure S10 shows the values of J (at –0.50 V) as a function of cycle number. The value of J for the junction with SC_9CH_3 was more stable than those junctions with SAMs of $SC_{13}CH_3$ (noisy around cycle number 975–985) and $SC_{17}CH_3$ (noisy for cycle number >1500). Figure 10b shows the retention characteristics of the devices. The junctions with SAMs of SC_9CH_3 and $SC_{13}CH_3$ were more stable than the junction with $SC_{17}CH_3$ which became noisy after 3.0×10^3 s. One possible reason for the difference in the electrical stability between the devices is that SAMs with long alkyl chains are more crystalline and therefore contain more defects from, for example, phase domains boundaries than the short liquid-like SAMs.[74,75] Figure 10c shows the J(V) curves of the device with SAMs of SC_9CH_3 determined at t = 0, 1, 2, 5, and 10 days. Over this period of time, the values of J decreased by approximately a factor of seven. A similar behavior was observed for devices with $SC_{13}CH_3$, and $SC_{17}CH_3$ SAMs (Figure S11, Supporting Information). The reason for the change in current densities is unclear, but it may involve oxidation of the metal-thiolate bonds[76–79] or the formation of silver sulfides.[80,81]

Measurements of J(V) as a function of temperature T (K) are important to establish the mechanism of charge transport across tunnel junctions. To test the stability of the devices against changes in temperature, we studied the electrical characteristics of the devices over a range of values of T of 160–297 K. These measurements were performed in a probe station at a pressure of 1×10^{-5} bar. In agreement with previous observations,[17] both the change of pressure from ambient to vacuum and solidification of the bulk EGaIn at T = 220–240 K did not result in shorts, open circuits, or changed the electrical characteristics of the devices notably in any other way. Figure 10d shows that the J(V) curves of devices with SAMs SC_9CH_3 are (almost) independent of temperature as expected when tunneling is the dominant mechanism of charge transport. The devices shorted at the temperature lower than 160 K likely due to the differences in the thermal expansion coefficients of the different components in the devices (3×10^{-4} K^{-1} for PDMS,[1] 0.08×10^{-4} K^{-1} for glass,[82] 0.042×10^{-4} K^{-1} for Ga_2O_3,[83] 0.18×10^{-4} K^{-1} for EGaIn).[84]

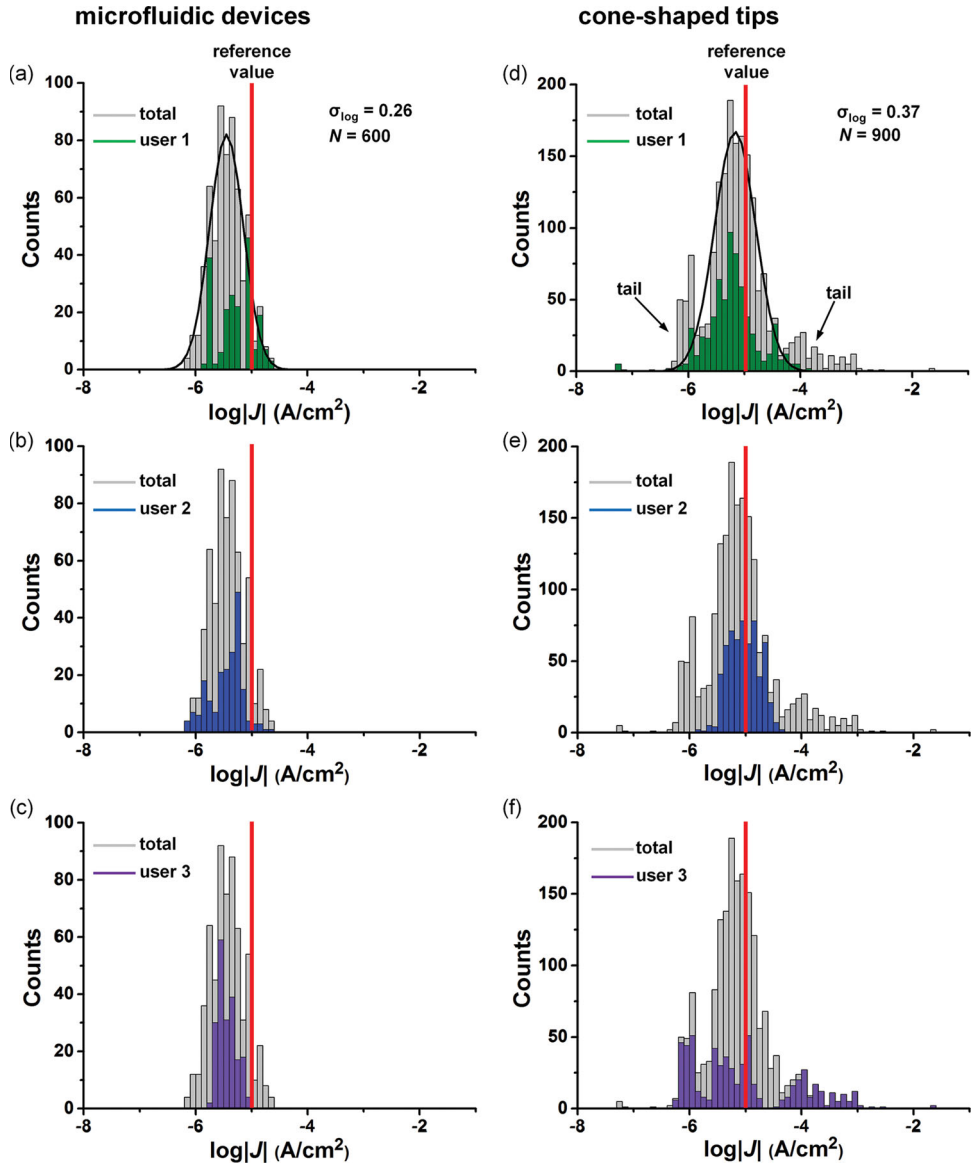

Figure 9. Histograms of the values of log|*J*| measured at –0.50 V for junctions with SAMs of $SC_{17}CH_3$ obtained by three different users a–c) using the same top-electrode or d–f) using conical tips of GaO_x/EGaIn. The red vertical line indicates the reference value of log|*J*| for Ag^{TS}-SC_{18}//GaO_x/EGaIn junctions.

3.8. Comparison to Other Test-Beds

To judge the performance of our method against previously reported test-beds, we compared i) yields in working junctions, ii) log-standard deviations as an indicator of reproducibility or precision, iii) values of β as an indicator of the replicability or quality of the junctions (lower or higher values than the consensus value of 0.9–1.1 n_C^{-1} are likely caused by artifacts),[13,16] and iv) the stability against voltage cycling (crudely judged from the number of scans), and v) the ability to generate statistically large numbers of data. Our fabrication technique give devices with i) yield larger than 75%, ii) values of σ_{log} smaller than 0.3, iii) β of 1.00 ± 0.03 n_C^{-1}, iv) good electrical stability (2500 times of voltage cycling), and v) produces statistically large numbers of data ($N > 600$). In Table 3 we highlighted techniques that have comparable or better characteristics than ours in bold. Although these criteria are arbitrary chosen and this comparison gives a crude impression at best how different test-beds perform relative to ours, this effort hopefully serves as a starting point to judge methods not only by yields in non-shorting junctions, or the value of β, but also by more criteria including stability and more importantly reproducibility and replicability.

Table 3 is not comprehensive, but we included data obtained by large-area SAM-based junctions that contain large numbers of molecules,[14,16,26,32,38–41,85–93] and techniques based on scanning probes[42,94,95] that contain small numbers of molecules or even single molecules. In typical scanning tunneling microscope (STM) measurements, the air or vacuum gap between the tip and the molecules complicates evaluating the true

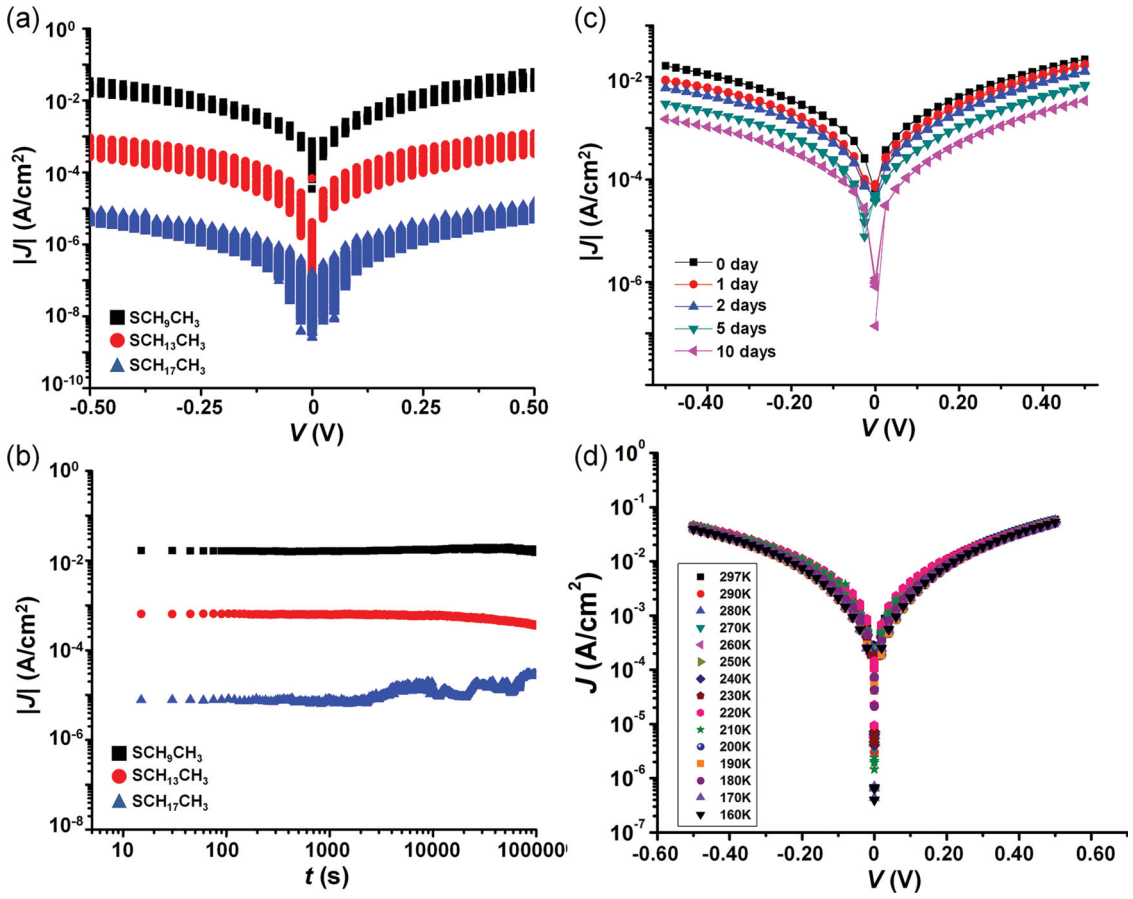

Figure 10. Stability of the junctions with SAMs of SC_9CH_3, $SC_{13}CH_3$ and $SC_{17}CH_3$. a) 2500 J(V) curves measured by continuously sweeping the bias between –0.50 and 0.50 V. b) Retention characteristics at a constant bias of –0.50 V for 27 h (bias was applied at $t = 0$ s and the current was measured at $t = 15$ s and onward at an interval of 15 s for 10^5 s). c) The J(V) curves of the devices with SAMs of SC_9CH_3 right after the devices were prepared and after aging up to ten days after which we stopped the experiment. d) The J(V) curves at different temperatures in the range of (160–297 K) for a junction with a SAM of SC_9CH_3.

conductance of the molecules.[14] The so-called STM break junction technique forms junctions by capturing the molecules between the STM tip and the bottom-electrode in situ from solution. Although this technique produces large numbers of data, little information is available regarding the supramolecular structure of the junctions. Direct deposition of the top-electrodes on SAMs resulted in low yields of non-shorting junctions and is prone to metal filament formation, and other types of defects.[26,96] Using a conductive layer (polymer[39,93] or graphene based materials)[87,91] between the SAM and the top-electrode protects the SAM during metal deposition and increased the yields. Other techniques have avoided metal deposition by using liquid-metal top-electrodes (Hg[32,38,41,88,97] or GaO_x/EGaIn)[40,47] which deform and conform to, rather than penetrate, the SAM once brought into contact with the SAM. Others have deposited solid electrodes from solution or used bending wires to form junctions.[86,89,90,92]

Among the methods that generate values of β that are close to 1.0 n_C^{-1}, our method has amongst the smallest σ_{log} values (0.12–0.25). Nanoskiving also generates comparably small σ_{log} values (≈0.05–0.28) with $\beta = 0.94$ n_C^{-1} but with low numbers of data.[85] Junctions with PDOT:PSS protection layers are generated in very high yields with small errors and good stabilities, but with very low values of β.[39,93] Junctions with graphene as protection layer perform also well and produce large numbers of data in high yields with β close to 1.0 n_C^{-1}, but with a larger error than our method.[87] For most fabrication methods, the stability of the junctions against voltage cycling has not been reported, but our method compares well in stability to that of the rigorously tested junctions with graphene protection layers.[87] Thus, we conclude that our fabrication method generates junctions with high reproducibility, replicability, good electrical stability, and generates statistically large numbers of data in good yields.

4. Conclusions

Here we report a new technique to from electrical top-contacts to SAMs that relies on a top-electrode of a non-Newtonian liquid metal alloy stabilized in a micro-scale through-hole in PDMS. This top-electrode can be directly placed onto the SAMs, removed from the SAMs once the measurements are completed, and used again to form a new junction. Typically 15–25 junctions can be formed with a single top-electrode.

Thus, this method provides the opportunity to investigate the reproducibility of the electrical characteristics of SAM-based junctions as a function of the top-electrodes and users. We found that the electrical characteristics are highly reproducible between different users and top-electrodes: the values of β obtained by three investigators using five different top-electrodes ranged only from 0.95 to 1.05 n_C^{-1} with an average value of 1.00 ± 0.03 n_C^{-1}.

Unlike other methods to fabricate SAM-based devices (of the sort shown in Figure 1), our technique is compatible with template-stripped bottom-electrodes and does not require patterning of the bottom-electrode. This ensures that the electrodes supporting the SAMs are clean and never had been exposed to photoresist (which is often difficult to remove completely)[28–31] and only briefly exposed to the ambient (few seconds),[35] and do not contain edges at which SAMs cannot pack well.[28–30] The stabilization of the top-electrode minimizes the user-to-user variation in contacting the SAMs, defines the geometrical area of the junctions. To improve replicability, prior to the SAM formation, we purified the thiols and characterized the template-stripped electrodes by AFM to confirm the quality of the bottom-electrodes. All these factors resulted in very narrow log-normally distributed values of J ($\sigma_{log} = 0.12 - 0.25$), i.e., the data generated by our junctions is highly reproducible in terms of precision with high replicability relative to other "EGaIn"-techniques.

This method minimizes the potential error associated with cone-shaped tips of GaO_x/EGaIn suspended from a syringe such as vibrations, pressure at which the tip is brought in contact with the SAM, or drift of the tip with respect to the SAM.[16,40,46] Therefore it is possible to measure J(V) curves over a range of temperatures of T = 160–297 K which confirmed that the dominant mechanism of charge transport is coherent tunneling. We conclude that all "EGaIn"-based techniques produce J(V) data that agree with one another (because the values of J_0 vary only a factor of ten which is small relative to the eight to nine orders of magnitude difference across text-beds), but our data are more precise (the distributions of J have small log-standard deviations; Table 1). To date we cannot explain the absolute values of the values of J (or J_0) in every detail. Whitesides et al.[46] reported that the GaO_x layer is highly conductive and does not affect J significantly, but the effective electrical contact area is smaller than the geometrical contact area and therefore results in an underestimation of the value of J_0. We will discuss the role of molecule-electrode contact resistances and defects on the values of J_0 elsewhere.[98]

The term "reproducibility" is ill-defined and so is the "quality" of SAM-based junctions. Therefore it is difficult to compare one test-bed to another, but by far most approaches have only focused on the yields in non-shorting junctions and standard deviations. We found that comparing yields and (log) standard deviations only provide marginal information regarding the quality of the junctions. For instance, techniques that produce significantly lower or higher values of β than 1.0 n_C^{-1} with very small standard deviations in high yields are perhaps precise, but are not accurate and likely probe defective junctions.[33] We used the following parameters to evaluate test-beds against each other: i) yields in non-shoring junctions (78%), ii) log-standard deviation (0.12–0.25), iii) value of β (1.00 ± 0.03 n_C^{-1}), iv) electrical stability (voltage cycling for 2500 cycles), and v) ability to generate large numbers of data (≥600). We found that our devices exhibit very good overall performance relative to other test-beds and that our junctions are of good quality and produce data that are both precise (Table 3) and replicable (relative to other "EGaIn"-based techniques; Table 1). Although this list is not exhaustive, we believe it serves as a good starting point to evaluate test-beds against each other.

Many fabrication methods use protective layers (to protect the SAMs during the metal deposition process to form the top-contacts) that are deposited by solution based processes, or on the deposition of the electrode from solution.[39,86,92] We believe that our method to form electrical contacts to SAMs of n-alkanethiolates can be readily extended to other types of SAMs, monolayers of biomolecules, or other types of materials that may not be compatible with direct deposition methods of metals, or exposure to solvents, to form high quality junctions in good yields with high reproducibility.

5. Experimental Section

Fabrication of the Ag^{TS} Substrates: The Ag substrates as the bottom-electrodes were prepared by template-stripped method as described in the literature.[32] The silver (purity of 99.999%) was purchased from Super Conductor Materials, Inc (USA). Si (100, p-type) wafers with thickness of 525 ± 25 μm were purchased from University Wafers (USA). We thermally evaporated a layer of 300 nm of Ag on the Si wafers at the pressure of around 2×10^{-6} mbar using a thermal evaporator (ShenYang KeYi, China). We deposited the first 50 nm of Ag at a rate of 0.5–0.7 Å s^{-1} followed by depositing another 250 nm of Ag at the rate of 1 Å s^{-1}. Glass slides cleaned with oxygen plasma were mounted on the Ag film by using photo-curable optical adhesive (OA, Norland, No. 61) as the adhesion layer. After photo-curing the optical adhesive for 1 h, the metal film around the glass slide was cut using a razor blade. The Ag film supported on the glass slide was lifted off from the Si wafer and immersed in the SAM solution in 5 s.

Formation of Alkanethiolate-SAMs on Ag^{TS}: The as-received n-alkanethiols (Sigma-Aldrich) were recrystallized from ethanol (AR grade) prior to use. The purities of the molecules after the recrystallization were determined by gas chromatography-mass spectroscopy (GC-MS, 7890A GC System/ 5975C Inert MSD, Agilent Technologies; see Supporting Information Figure S12 and Table S1). All purified thiols were kept under N_2 atmosphere at 4 °C to avoid the reaction between atmospheric O_2 and the thiols. The template-stripped silver (Ag^{TS}) supported on glass slide was immersed in n-alkanethiol solutions (3.0 mM in absolute ethanol) for three hours in a glass vial filled with N_2. The n-alkanethiol solution was degassed by N_2 for 10 min prior to the immersion of the Ag^{TS} substrates. After the formation of SAMs, the substrate was cleaned with copious amounts of ethanol to remove physisorbed molecules and was blown to dryness in a stream of N_2.

Imaging: The surface roughness and the grain size of the Ag^{TS} and as-deposited Ag substrates were determined by using tapping-mode AFM (Dimension Fastscan). The AFM images with area of 1 μm × 1 μm were acquired and were further analyzed by using the Nanoscope software. The optical micrographs were acquired using an optical microscope (LEICA DM 2500M). We placed the top-electrode on a piece of ITO substrate and then flipped the substrate over under the objective of the microscope to observe the bottom-view of the top-electrode and determined the contact area between GaO_x/EGaIn and the substrate. The image of the mold made of photoresist on Si was measured using a SEM (JOEL JSM 6701F) under an accelerating voltage of 5 kV. The sample was sputter-coated with 5 nm of Au prior to the measurement to avoid charging effects during the image acquisition.

Electrical Measurements: The electrical measurements for the junctions in the devices were conducted by placing the top-electrode on the SAM-Ag^{TS} substrate, and forming the contact between the GaO_x/EGaIn at the inlet of the channel of the top-electrode and a tungsten probe (Signatone, SE-T) mounted on a micromanipulator (Signatone, S-725-PLM) while another probe was positioned on the substrate. Both probes were connected to a Keithley 6430 source meter. In our measurements, we biased the GaO_x/EGaIn and grounded the Ag substrates through the source meter and shielded cables. The J(V,T) measurements were carried out in a probe station (Lakeshore CRX-VF) at a pressure of $\approx 3 \times 10^{-5}$ bar. A code written in LabView 2010 was used to operate the source meter and recorded the J(V) curves.

Supporting Information

Supporting Information is available from the Wiley Online Library or from the author.

Acknowledgements

A.W. and L.J. contributed equally to this work. The authors gratefully acknowledge the Singapore National Research Foundation (NRF) for financial support under CRP award No. NRF-CRP8–2011–07.

Received: December 20, 2013
Revised: February 19, 2014
Published online: April 16, 2014

[1] S. R. Forrest, *Nature* **2004**, *428*, 911.
[2] G. Gelinck, P. Heremans, K. Nomoto, T. D. Anthopoulos, *Adv. Mater.* **2010**, *22*, 3778.
[3] J. Shinar, R. Shinar, *J. Phys. D: Appl. Phys.* **2008**, *41*, 1.
[4] O. Prache, *Displays* **2001**, *22*, 49.
[5] S. Chen, L. Deng, J. Xie, L. Peng, L. Xie, Q. Fan, W. Huang, *Adv. Mater.* **2010**, *22*, 5227.
[6] T. W. Kelley, P. F. Baude, C. Gerlach, D. E. Ender, D. Muyres, M. A. Haase, D. E. Vogel, S. D. Theiss, *Chem. Mater.* **2004**, *16*, 4413.
[7] S. Park, G. Wang, B. Cho, Y. Kim, S. Song, Y. Ji, M.-H. Yoon, T. Lee, *Nat. Nanotechnol.* **2012**, *7*, 438.
[8] J. Lewis, *Mater. Today* **2006**, *9*, 38.
[9] G. Wang, T. W. Kim, T. Lee, *J. Mater. Chem.* **2011**, *21*, 18117.
[10] C. C. Jia, X. F. Guo, *Chem. Soc. Rev.* **2013**, *42*, 5642.
[11] M. Kiguchi, S. Kaneko, *ChemPhysChem* **2012**, *13*, 1116.
[12] L. A. Luo, S. H. Choi, C. D. Frisbie, *Chem. Mater.* **2011**, *23*, 631.
[13] H. B. Akkerman, B. de Boer, *J. Phys.: Condens. Mat.* **2008**, *20*, 1.
[14] H. Song, M. A. Reed, T. Lee, *Adv. Mater.* **2011**, *23*, 1583.
[15] H. Haick, D. Cahen, *Prog. Surf. Sci.* **2008**, *83*, 217.
[16] C. A. Nijhuis, W. F. Reus, J. R. Barber, G. M. Whitesides, *J. Phys. Chem. C* **2012**, *116*, 14139.
[17] C. A. Nijhuis, W. F. Reus, J. R. Barber, M. D. Dickey, G. M. Whitesides, *Nano Lett.* **2010**, *10*, 3611.
[18] C. P. Collier, E. W. Wong, M. Belohradsky, F. M. Raymo, J. F. Stoddart, P. J. Kuekes, R. S. Williams, J. R. Heath, *Science* **1999**, *285*, 391.
[19] R. P. Kalakodimi, A. M. Nowak, R. L. McCreery, *Chem. Mater.* **2005**, *17*, 4939.
[20] R. L. McCreery, J. Wu, R. P. Kalakodimi, *Phys. Chem. Chem. Phys.* **2006**, *8*, 2572.
[21] R. M. Metzger, B. Chen, U. Hopfner, M. V. Lakshmikantham, D. Vuillaume, T. Kawai, X. L. Wu, H. Tachibana, T. V. Hughes, H. Sakurai, J. W. Baldwin, C. Hosch, M. P. Cava, L. Brehmer, G. J. Ashwell, *J. Am. Chem. Soc.* **1997**, *119*, 10455.
[22] J. Chen, M. A. Reed, A. M. Rawlett, J. M. Tour, *Science* **1999**, *286*, 1550.
[23] W. Y. Wang, T. Lee, I. Kretzschmar, M. A. Reed, *Nano Lett.* **2004**, *4*, 643.
[24] W. Y. Wang, T. Lee, M. A. Reed, *Rep. Prog. Phys.* **2005**, *68*, 523.
[25] G. Wang, T. W. Kim, H. Lee, T. Lee, *Phys. Rev. B* **2007**, *76*, 205320.
[26] T. W. Kim, G. N. Wang, H. Lee, T. Lee, *Nanotechnology* **2007**, *18*, 315204.
[27] G. Wang, T. W. Kim, Y. H. Jang, T. Lee, *J. Phys. Chem. C* **2008**, *112*, 13010.
[28] J. Cantone, Y. van Dommelen, A. Q. Jiang, S. Dunn, T. Winter, K. Petrillo, R. Johnson, P. Lawson, W. Conley, R. Callahan, *J. Vac. Sci. Technol. B* **2009**, *27*, 3014.
[29] H. Y. Mao, D. Wu, W. G. Wu, J. Xu, Y. L. Hao, *Nanotechnology* **2009**, *20*, 445304–445309.
[30] M. S. Chen, S. L. Brandow, W. J. Dressick, *Thin Solid Films* **2000**, *379*, 203.
[31] M. S. Chen, S. L. Brandow, C. S. Dulcey, W. J. Dressick, G. N. Taylor, J. F. Bohland, J. H. G. Georger, E. K. Pavelchek, J. M. Calvert, *J. Electrochem. Soc.* **1999**, *146*, 1421.
[32] E. A. Weiss, R. C. Chiechi, G. K. Kaufman, J. K. Kriebel, Z. F. Li, M. Duati, M. A. Rampi, G. M. Whitesides, *J. Am. Chem. Soc.* **2007**, *129*, 4336.
[33] L. Yuan, L. Jiang, B. Zhang, C. A. Nijhuis, *Angew. Chem. Int. Ed.* **2014**, *53*, 3377.
[34] J. C. Love, L. A. Estroff, J. K. Kriebel, R. G. Nuzzo, G. M. Whitesides, *Chem. Rev.* **2005**, *105*, 1103.
[35] E. A. Weiss, G. K. Kaufman, J. K. Kriebel, Z. Li, R. Schalek, G. M. Whitesides, *Langmuir* **2007**, *23*, 9686.
[36] J. Deng, W. Hofbauer, N. Chandrasekhar, S. J. O'Shea, *Nanotechnology* **2007**, *18*, 155202.
[37] J. M. Beebe, J. G. Kushmerick, *Appl. Phys. Lett.* **2007**, *90*, 083117.
[38] R. L. York, P. T. Nguyen, K. Slowinski, *J. Am. Chem. Soc.* **2003**, *125*, 5948.
[39] G. Wang, H. Yoo, S. I. Na, T. W. Kim, B. Cho, D. Y. Kim, T. Lee, *Thin Solid Films* **2009**, *518*, 824.
[40] M. M. Thuo, W. F. Reus, C. A. Nijhuis, J. R. Barber, C. Kim, M. D. Schulz, G. M. Whitesides, *J. Am. Chem. Soc.* **2011**, *133*, 2962.
[41] I. Levine, S. M. Weber, Y. Feldman, T. Bendikov, H. Cohen, D. Cahen, A. Vilan, *Langmuir* **2012**, *28*, 404.
[42] V. B. Engelkes, J. M. Beebe, C. D. Frisbie, *J. Am. Chem. Soc.* **2004**, *126*, 14287.
[43] W. F. Reus, C. A. Nijhuis, J. R. Barber, M. M. Thuo, S. Tricard, G. M. Whitesides, *J. Phys. Chem. C* **2012**, *116*, 6714.
[44] ISO, Replicability (Trueness and Precision) of Measurement Methods and Results: General Principles and Definitions/Part 1, International Organization for Standardization Geneva, Switzerland, **1994**.
[45] R. L. McCreery, A. J. Bergren, *Adv. Mater.* **2009**, *21*, 4303.
[46] F. C. Simeone, H. J. Yoon, M. M. Thuo, J. R. Barber, B. Smith, G. M. Whitesides, *J. Am. Chem. Soc.* **2013**, *135*, 18131.
[47] L. Cademartiri, M. M. Thuo, C. A. Nijhuis, W. F. Reus, S. Tricard, J. R. Barber, R. N. S. Sodhi, P. Brodersen, C. Kim, R. C. Chiechi, G. M. Whitesides, *J. Phys. Chem. C* **2012**, *116*, 10848.
[48] R. C. Chiechi, E. A. Weiss, M. D. Dickey, G. M. Whitesides, *Angew. Chem. Int. Ed.* **2008**, *47*, 142.
[49] D. Fracasso, H. Valkenier, J. C. Hummelen, G. C. Solomon, R. C. Chiechi, *J. Am. Chem. Soc.* **2011**, *133*, 9556.
[50] N. Nerngchamnong, L. Yuan, D. C. Qi, J. Li, D. Thompson, C. A. Nijhuis, *Nat. Nanotechnol.* **2013**, *8*, 113.
[51] S. Ramachandra, K. C. Schuermann, F. Edafe, P. Belser, C. A. Nijhuis, W. F. Reus, G. M. Whitesides, L. De Cola, *Inorg. Chem.* **2011**, *50*, 1581.
[52] W. F. Reus, M. M. Thuo, N. D. Shapiro, C. A. Nijhuis, G. M. Whitesides, *ACS Nano* **2012**, *6*, 4806.

[53] C. A. Nijhuis, W. F. Reus, A. C. Siegel, G. M. Whitesides, *J. Am. Chem. Soc.* **2011**, *133*, 15397.
[54] C. A. Nijhuis, W. F. Reus, G. M. Whitesides, *J. Am. Chem. Soc.* **2009**, *131*, 17814.
[55] D. Fracasso, M. I. Muglali, M. Rohwerder, A. Terfort, R. C. Chiechi, *J. Phys. Chem. C* **2013**, *117*, 11367.
[56] M. M. Thuo, W. F. Reus, F. C. Simeone, C. Kim, M. D. Schulz, H. J. Yoon, G. M. Whitesides, *J. Am. Chem. Soc.* **2012**, *134*, 10876.
[57] H. J. Yoon, N. D. Shapiro, K. M. Park, M. M. Thuo, S. Soh, G. M. Whitesides, *Angew. Chem. Int. Ed.* **2012**, *51*, 4658.
[58] K. Smaali, S. Lenfant, S. Karpe, M. Oçafrain, P. Blanchard, D. Deresmes, S. Godey, A. Rochefort, J. Roncali, D. Vuillaume, *ACS Nano* **2010**, *4*, 2411.
[59] A. M. Masillamani, N. Crivillers, E. Orgiu, J. Rotzler, D. Bossert, R. Thippeswamy, M. Zharnikov, M. Mayor, P. Samori, *Chem. Eur. J.* **2012**, *18*, 10335.
[60] S. J. French, D. J. Saunders, G. W. Ingle, *J. Phys. Chem.* **1938**, *42*, 265.
[61] J. Thelen, M. D. Dickey, T. Ward, *Lab Chip* **2012**, *12*, 3961.
[62] K. P. Mineart, Y. L. Lin, S. C. Desai, A. S. Krishnan, R. J. Spontak, M. D. Dickey, *Soft Mater.* **2013**, *9*, 7695.
[63] E. P. Kartalov, C. Walker, C. R. Taylor, W. F. Anderson, A. Scherer, *Proc. Natl. Acad. Sci. U.S.A.* **2006**, *103*, 12280.
[64] G. J. Hayes, J. H. So, A. Qusba, M. D. Dickey, G. Lazzi, *IEEE T. Antenn. Propag.* **2012**, *60*, 2151.
[65] M. D. Dickey, R. C. Chiechi, R. J. Larsen, E. A. Weiss, D. A. Weitz, G. M. Whitesides, *Adv. Funct. Mater.* **2008**, *18*, 1097.
[66] J. C. McDonald, D. C. Duffy, J. R. Anderson, D. T. Chiu, H. K. Wu, O. J. A. Schueller, G. M. Whitesides, *Electrophoresis* **2000**, *21*, 27.
[67] J. Aizenberg, A. J. Black, G. M. Whitesides, *Nature* **1998**, *394*, 868.
[68] C. A. Nijhuis, W. F. Reus, G. M. Whitesides, *J. Am. Chem. Soc.* **2010**, *132*, 18386.
[69] M. T. Cygan, T. D. Dunbar, J. J. Arnold, L. A. Bumm, N. F. Shedlock, T. P. Burgin, L. Jones, D. L. Allara, J. M. Tour, P. S. Weiss, *J. Am. Chem. Soc.* **1998**, *120*, 2721.
[70] T. Lee, W. Y. Wang, J. F. Klemic, J. J. Zhang, J. Su, M. A. Reed, *J. Phys. Chem. B* **2004**, *108*, 8742.
[71] S. Ssenyange, H. J. Yan, R. L. McCreery, *Langmuir* **2006**, *22*, 10689.
[72] E. Kokkoli, C. F. Zukoski, *J. Colloid Interface Sci.* **1999**, *209*, 60.
[73] D. Käfer, G. Witte, P. Cyganik, A. Terfort, C. Woll, *J. Am. Chem. Soc.* **2006**, *128*, 1723.
[74] M. D. Porter, T. B. Bright, D. L. Allara, C. E. D. Chidsey, *J. Am. Chem. Soc.* **1987**, *109*, 3559.
[75] S. D. Evans, A. Ulman, *Chem. Phys. Lett.* **1990**, *170*, 462.
[76] T. M. Willey, A. L. Vance, T. van Buuren, C. Bostedt, L. J. Terminello, C. S. Fadley, *Surf. Sci.* **2005**, *576*, 188.
[77] Y. Z. Li, J. Y. Huang, R. T. McIver, J. C. Hemminger, *J. Am. Chem. Soc.* **1992**, *114*, 2428.
[78] M. J. Tarlov, D. R. F. Burgess, G. Gillen, *J. Am. Chem. Soc.* **1993**, *115*, 5305.
[79] M. H. Schoenfisch, J. E. Pemberton, *J. Am. Chem. Soc.* **1998**, *120*, 4502.
[80] P. E. Laibinis, G. M. Whitesides, D. L. Allara, Y. T. Tao, A. N. Parikh, R. G. Nuzzo, *J. Am. Chem. Soc.* **1991**, *113*, 7152.
[81] J. P. Franey, G. W. Kammlott, T. E. Graedel, *Corros. Sci.* **1985**, *25*, 133.
[82] E. A. Weiss, G. K. Kaufman, J. K. Kriebel, Z. Li, R. Schalek, G. M. Whitesides, *Langmuir* **2007**, *23*, 9686.
[83] E. P. Kartalov, C. Walker, C. R. Taylor, W. F. Anderson, A. Scherer, *Proc. Natl. Acad. Sci. U.S.A.* **2006**, *103*, 12280.
[84] N. Bowden, W. T. S. Huck, K. E. Paul, G. M. Whitesides, *Appl. Phys. Lett.* **1999**, *75*, 2557.
[85] P. Pourhossein, R. C. Chiechi, *ACS Nano* **2012**, *6*, 5566.
[86] S. O. Krabbenborg, J. G. E. Wilbers, J. Huskens, W. G. van der Wiel, *Adv. Funct. Mater.* **2013**, *23*, 770.
[87] G. Wang, Y. Kim, M. Choe, T. W. Kim, T. Lee, *Adv. Mater.* **2011**, *23*, 755.
[88] O. Yaffe, Y. B. Qi, L. Scheres, S. R. Puniredd, L. Segev, T. Ely, H. Haick, H. Zuilhof, A. Vilan, L. Kronik, A. Kahn, D. Cahen, *Phys. Rev. B* **2012**, *85*, 045433.
[89] M. Coll, N. Gergel-Hackett, C. A. Richter, C. A. Hacker, *J. Phys. Chem. C* **2011**, *115*, 24353.
[90] J. G. Kushmerick, D. B. Holt, S. K. Pollack, M. A. Ratner, J. C. Yang, T. L. Schull, J. Naciri, M. H. Moore, R. Shashidhar, *J. Am. Chem. Soc.* **2002**, *124*, 10654.
[91] S. Seo, M. Min, S. M. Lee, H. Lee, *Nat. Commun.* **2013**, *4*, 1920.
[92] N. Stein, R. Korobko, O. Yaffe, R. H. Lavan, H. Shpaisman, E. Tirosh, A. Vilan, D. Cahen, *J. Phys. Chem. C* **2010**, *114*, 12769.
[93] H. B. Akkerman, P. W. M. Blom, D. M. de Leeuw, B. de Boer, *Nature* **2006**, *441*, 69.
[94] C. Li, I. Pobelov, T. Wandlowski, A. Bagrets, A. Arnold, F. Evers, *J. Am. Chem. Soc.* **2008**, *130*, 318.
[95] T. Kirn, H. M. S. Hybertsen, L. Venkataraman, *Nano Lett.* **2013**, *13*, 3358.
[96] H. Song, T. Lee, N. J. Choi, H. Lee, *Appl. Phys. Lett.* **2007**, *91*, 253116.
[97] Y. Selzer, A. Salomon, D. Cahen, *J. Am. Chem. Soc.* **2002**, *124*, 2886.
[98] J. Li, C. S. S. Sangeeth, A. Wan, C. A. Nijhuis, unpublished.